CONF-8910225--2

* The submitted manuscript has been authored by a contractor of the U S Government under contract No DE-AC05-84OR21400. Accordingly, the U S Government retains a nonexclusive, royalty-free license to publish or reproduce the published form of this contribution, or allow others to do so, for U S Government purposes

DETERMINATION OF ICRF ANTENNA FIELDS IN THE VICINITY OF A 3-D FARADAY SHIELD STRUCTURE*

P.M. Ryan, K.E. Rothe, J.H. Whealton, and T.D. Shepard
Oak Ridge National Laboratory, Oak Ridge, TN 37831

CONF-8910225--2
DE90 001354

ABSTRACT

A three-dimensional (3-D) magnetostatic analysis developed at Oak Ridge National Laboratory has been used to calculate the electromagnetic transmission properties of representative Faraday shield designs. The analysis uses the long-wavelength approximation to obtain a 3-D Laplace solution for the magnetic scalar potential over one poloidal period of the Faraday shield, from which the complete magnetic field distribution may be obtained. Once the magnetic field distributions in the presence and absence of a Faraday shield are known, the flux transmission coefficient can be found, as well as any change in the distributed inductance of the current strap. The distributed capacitance of the strap can be found from an analogous 3-D electrostatic calculation, enabling the phase velocity of the slow-wave structure to be determined. Power dissipation in the shield may be estimated by equating the surface current on a perfect conductor with the surface magnetic field and using this surface current in conjunction with the finite conductivities of the shield materials to obtain the power distribution due to eddy current heating.

I. INTRODUCTION

The Faraday shield is an integral part of an ICRH antenna, and its design has fundamental consequences on the antenna performance. The purpose of a Faraday shield is essentially three-fold: (1) to protect the antenna from line-of-sight radiation from the plasma; (2) to exclude plasma from the immediate environment of the current strap; and (3) to reduce the electrostatic coupling between the current strap and the plasma. The antenna designer needs to know the effect of a Faraday shield design on the antenna performance: its power transmission, its power dissipation, and its effect on the antenna inductance and capacitance. The following analysis was developed to answer these questions and in doing so provides information about the vacuum fields in the vicinity of the shield.

*Research sponsored by the Office of Fusion Energy, U.S. Department of Energy, under contract DE-AC05-84OR21400 with Martin Marietta Energy Systems, Inc.

MASTER

II. THE 3-D MAGNETOSTATIC MODEL

The analysis starts with the differential form of Ampère's law, Fourier-analyzed in time and space:

$$\nabla \times \mathbf{B} = -j\,\mathbf{k} \times \mathbf{B} = \mu_0 \mathbf{J} + j\omega\mu_0\varepsilon_0 \mathbf{E} = j\left(k_0/c\right)\mathbf{E}, \tag{1}$$

where the current density **J** vanishes in the solution domain; that is, no volume currents are considered and the surface currents flowing on the current strap and cavity walls are consequences of the boundary conditions imposed on the problem. Equation (1) can be further simplified by applying the long-wavelength approximation, which is applicable when $k_0/k \approx h/\lambda \ll 1$, where h is the characteristic scale length of the device and λ is a free-space wavelength. In the case of our Faraday shield model, this approximation is equivalent to stating that the free-space wavelength (typically on the order of meters) is much larger than the poloidal period of the Faraday shield (typically on the order of a centimeter or less), so that over this poloidal distance the current and voltage on the current strap are essentially constant. This approximation decouples the electric and magnetic fields and reduces Eq. (1) to the curl-free static representation,

$$\nabla \times \mathbf{B} = 0. \tag{2}$$

This allows **B** to be defined as the gradient of a scalar potential Ψ_m, which is a solution of Laplace's equation,

$$\nabla \cdot \mathbf{B} = \nabla \cdot \left(\nabla \Psi_m\right) = \nabla^2 \Psi_m = 0. \tag{3}$$

It is worth noting here that the long-wavelength approximation is not exactly equivalent to the low-frequency or quasistatic approximation, in which the frequency is set to zero. We retain a nonzero frequency in order to impose proper boundary conditions on the conducting surfaces; we note there can be no time-varying magnetic field inside a perfect conductor. By imposing Neumann boundary conditions on Ψ_m at all conducting surfaces, we ensure that the normal component of **B** vanishes at the surface.

The integral form of Ampère's law, which equates the total current flowing in the strap with the line integral of **B** along any contour that encloses the strap, is used to set the Dirichlet boundary conditions on the remaining symmetry surfaces:

$$\oint_c \mathbf{B} \cdot d\mathbf{l} = 2\int_{c\Omega} \nabla \Psi_m \cdot d\mathbf{l} = 2\left(\Psi_{m2} - \Psi_{m1}\right) = \mu_0 I_{\text{strap}}, \tag{4}$$

where $\Psi_{m1} \equiv 0$ and $\Psi_{m2} \equiv \mu_0 I_{strap}/2$. The total current in the strap is therefore determined by the magnetostatic potential that is applied to the symmetry plane. The current distribution on the strap, which is equivalent to the surface magnetic field, is not specified but is determined self-consistently from the gradient of the magnetostatic potential,

$$\mu_0 \mathbf{J}_{strap} = \mathbf{n} \times \mathbf{B} = \mathbf{n} \times \nabla \Psi_m . \tag{5}$$

The flux transmission efficiency is determined by comparing the magnetic field calculated with the Faraday shield in place to the field obtained in the absence of the Faraday shield; the current is kept constant in the current strap for the two cases.

The presence of the Faraday shield can reduce the strap inductance, hence reducing the amount of flux produced for a given strap current. The strap inductance per unit length, L', can be determined by applying Faraday's law to the magnetic flux, ψ, that passes through the symmetry plane between the current strap and the rear wall of the cavity to obtain the voltage per unit length along the strap, V', and equating it to that obtained from circuit theory,

$$V' = -j\omega \int_S \mathbf{B} \cdot d\mathbf{S} = -j\omega\psi = j\omega L' I_{strap} \tag{6}$$

$$L' = -\frac{\psi}{I_{strap}} . \tag{7}$$

The Faraday shield has much greater influence on the strap capacitance than on the strap inductance, increasing it considerably over the value obtained with no shield in place. The current strap/Faraday shield combination is a periodic slow-wave structure whose phase velocity is lower than the speed of light in vacuum. A lower phase velocity results in a shorter wavelength along the antenna; that is, the antenna is electrically longer with the Faraday shield in place. The shorter wavelength produces a greater deviation from constant current along the strap, which reduces the total power radiated by the antenna for a given maximum strap current. On the other hand, the reduction in inductance also reduces the maximum strap voltage encountered for the same strap current.

The capacitance of one poloidal period of the current strap may be calculated from a 3-D electrostatic model. Here again we use the long-wavelength approximation to assume that the strap voltage is constant over one poloidal period. We again solve Laplace's equation, but this time for the electrostatic potential Φ,

$$\nabla^2 \Phi = 0, \tag{8}$$

subject to the boundary conditions that $\Phi = \Phi_0$ on the current strap and $\Phi = 0$ on other metallic boundaries. Neumann boundary conditions are applied to the three symmetry planes of the top, the bottom (poloidal periodicity), and the plane bisecting the current strap. The strap capacitance is found from the definition of capacitance and the boundary condition on the normal component of the electric field at the surface of a perfect conductor

$$C' = \frac{Q}{V}, \tag{9}$$

$$\rho_s = \mathbf{n} \cdot \mathbf{E} = \mathbf{n} \cdot \nabla\Phi, \tag{10}$$

$$C' = \frac{\int_S \mathbf{n} \cdot \nabla\Phi \, dS}{\Phi_0}, \tag{11}$$

where the surface electric field is integrated on the entire strap surface. The phase velocity v_p and the characteristic impedance Z_0 of the current strap can then be determined from transmission-line theory as

$$v_p = (L'C')^{-1/2} \tag{12}$$

$$Z_0 = \left(L'/C'\right)^{1/2}. \tag{13}$$

III. CALCULATIONS AND COMPARISON WITH MEASUREMENTS

Some of the Faraday shield designs that have been considered are shown in Fig. 1. The "single-tier triangular" and the "double-tier Perkins" were tested on a mock-up antenna. The "ORNL C-MOD" geometry has been proposed for the ORNL antenna design for Alcator C-MOD and is similar to shield #10, which was tested on a functional development antenna [1] along with the "ASDEX" shield. The "MIT C-MOD" geometry will be used on the antenna designed by the Massachusettes Institute of Technology for Alcator C-MOD [2]. It has been speculated that shields of triangular cross-section may ameliorate the transport into the plasma of impurity ions sputtered from the shield [3]; proper design and orientation may decrease the impurity generation rate as well.

The 3-D Laplace boundary value problem is numerically solved with a modified version of the ORNL Vlasov-Poisson finite-difference code [4]. Figure 2 shows the top view and side view of a typical cavity/strap/shield geometry; the structure extends poloidally for one Faraday shield period. The 3-D structure is divided toroidally into a

finite number of discrete planes, each plane containing a cross-section of the shield. The dotted lines in Fig. 2 represent the symmetry planes where the Dirichlet boundary conditions are imposed; the magnitude of the nonzero constant potential surface is directly proportional to the strap current. All the solid lines represent Neumann boundaries, either perfectly conducting or poloidally symmetric surfaces, where the normal component of the magnetic field vanishes. The grid spacing for the finite-difference mesh in the plane of the shield cross-section was typically 0.04 to 0.10 cm in order to approximate the actual shield geometry as closely as possible. The grid spacing in the third dimension is not as critical as far as geometric resolution is concerned; however, the coupling in this dimension must be large enough (spacing small enough) to minimize numerical inaccuracies and to speed convergence. Mesh spacing of 0.4 to 0.5 cm was typical; this yields about 100,000 nodes on which the magnetic potential must be solved.

The numerical results for power transmission and effect on inductance and capacitance are shown in Table I and compared with measurements where possible. Three different cavity/strap geometries were chosen to correspond with the dimensions of the mock-up antenna, the development antenna, and a nominal C-MOD antenna. The magnetic field attenuation caused by the Faraday shield is not greatly affected by the strap/cavity geometry, although the changes in inductance and capacitance are. The square of the magnetic field is evaluated at a given radial distance from the strap both with and without the Faraday shield in order to calculate the power transmission coefficient; the strap current is kept constant.

The mock-up antenna was provided with an absorbent rf load and driven by the reference port of a network analyzer. A small loop probe aligned with the toroidal field component was positioned near the load and connected to the test port of the analyzer. The calculation of the transmission coefficient consists of measuring the forward gain with and without the presence of the Faraday shield; the change in the antenna input impedance needs to be taken into account:

$$T_F = \frac{(V_{Test}/V_{in})_{FS}}{(V_{Test}/V_{in})_{No\,FS}} \frac{(Z_{in})_{FS}}{(Z_{in})_{No\,FS}} . \tag{14}$$

The measured power transmission includes the power dissipation in the shield while the calculated power transmission does not. The effective power transmission appearing in Table I is the calculated power transmission minus the shield dissipation,

$$(T_p)\text{eff} = \frac{(P_{Load})_{FS}}{(P_{Load})_{No\,FS}} = (T_p)\text{calc} - \frac{R_{FS}}{R_L}. \tag{15}$$

The correction is greatest for those shields with large rf resistances, which are typically designs possessing narrow gaps, sharp corners, and/or poor conducting material in the regions of high currents.

IV. POWER DISSIPATION IN FARADAY SHIELDS

The tangential component of **B** is not compressed but is continuous across the shield, as is seen in Fig. 3a (the slight increase in the tangential field between the front and rear tiers is due to reflections, not compression). This tangential component of the field will induce surface currents (constant in magnitude) to flow around the circumference of the shield. The normal components of **B** cannot pass through the conducting surface of the Faraday shield. Eddy currents are induced that cancel out **B** normal to the surface and generate a component that is parallel to the surface. These longitudinally directed currents give rise to a poloidal component of **B** that did not exist in the absence of the shield, which in turn allows the magnetic field to flow around the tube and into the shield gap. Figure 3b shows that the normal (radial) magnetic field has been compressed and the maximum occurs at the narrowest restriction, which is where the longitudinal surface currents and power dissipation are also the highest.

The effect of the shield geometry on power dissipation can be modeled most accurately with a two-dimensional treatment using input from the 3-D calculations. This allows the finite-difference grid to be more dense in the vicinity of the Faraday shield. An example of the compression of the radial flux is shown in Fig. 4 for an ORNL C-MOD shield design in which the surface of the front tier of the shield has been flattened to reduce the total shield thickness. The longitudinal surface currents are proportional to the flux density at the surface (the gradient of the potential contours). The field enhancement $\gamma(s)$ is defined as the ratio of the normal surface fields along the shield circumference to the radial field in the absence of the shield. The average longitudinal power dissipation per poloidal period at a

point along the shield is then

$$\langle P \rangle = \frac{1}{2}\oint_C \eta J_{surf}^2(s)ds = \frac{\eta\delta}{4}\oint_C \gamma^2(s)B_\perp^2 + B_\parallel^2 ds \tag{16}$$

where η is the resistivity of the material, δ is the skin depth, $B_\perp$ and $B_\parallel$ are the perpendicular and parallel field components in the absence of the shield, and the integration is carried out over the circumference of the shield cross-section.

Figure 5 shows the power deposited in the ORNL C-MOD shield, divided between the two field components. Figure 5a plots $B_\perp^2$, $B_\parallel^2$, and their sum in the absence of flux compression, while Fig. 5b plots them with flux compression. It can be seen that the normal magnetic field component is primarily responsible for shield heating. It is peaked along the front of the shield near the end of the current strap, where the radial flux is the largest, and along the side of the shield where it is attached to the cavity wall.

REFERENCES

[1] D.J. Hoffman et al., Fusion Technol. **8**, 392 (1985).

[2] Y. Takase et al., AIP Conf. Proc. **190** (RF Power in Plasmas, Irvine, CA), 346 (1989).

[3] F.W. Perkins, PPPL Report 2571 (1988).

[4] P.M. Ryan et al., AIP Conf. Proc. **190** (RF Power in Plasmas, Irvine, CA), 322 (1989).

FIGURE CAPTIONS

Fig. 1. Cross sections of five Faraday shields that were analyzed; the single-tier triangular and the double tier "Perkins" were tested on a mock-up antenna.

Fig. 2. Top and side views of a typical cavity used in the 3-D calculations; actual cavity geometries used for each shield are listed in Table I.

Fig. 3. (a) The toroidal field component at the midplane of the cavity; the circles are with the Faraday shield ORNL C-MOD in Fig. 1, and the solid line is the field with no shield. (b) The radial field component near the side wall of the cavity, again with and without a Faraday shield.

Fig. 4. Example of the compression of the radial magnetic flux in the gap of the ORNL C-MOD shield; the side facing the plasma has been flattened to reduce the shield width.

Fig. 5. (a) The average power distribution along a Faraday shield that extends across the front and around the side of the current strap; the dark circles arise from the rotational currents, the light circles arise from the longitudinal currents (normal fields assumed uncompressed), and the solid line is their sum. (b) The average power distribution when the compression of the normal field component is taken into account.

COMPARISON OF CALCULATIONS WITH MEASUREMENTS

GEOMETRY	SINGLE TIER TRIANGULAR	DOUBLE TIER "PERKINS"	ORNL CMOD (Shield #10)	MIT CMOD	"ASDEX"
Transmission (T_F)					
Measured	0.804	0.749	0.897	-	0.767
Calculated	0.883	0.835	0.915	0.819	0.831
Power Trans. (T_P)					
Measured	0.646	0.561	0.805	-	0.588
Calculated	0.775	0.697	0.840	0.667	0.687
Effective	0.718	0.583	-	-	-
$\Delta L'/L'$					
Measured	-3.0%	-3.7%	-7.5%	-	-9.6%
Calculated	-1.3%	-1.8%	-9.0%	-15.7%	-8.1%
$\Delta C'/C'$					
Calculated	+24.5%	+23.4%	+109%	-	-

Table I

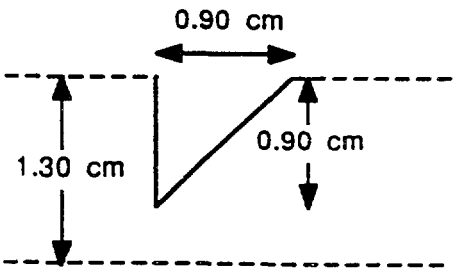

SINGLE TIER TRIANGULAR

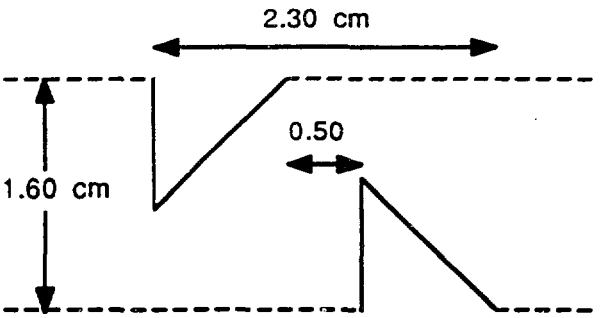

DOUBLE TIER "PERKINS"

(Perkins, PPPL Report 2571)

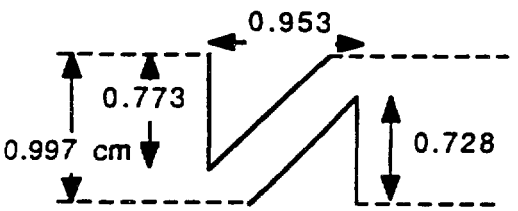

MIT C-MOD

(Takase, et al, AIP Conf 190, p. 346)

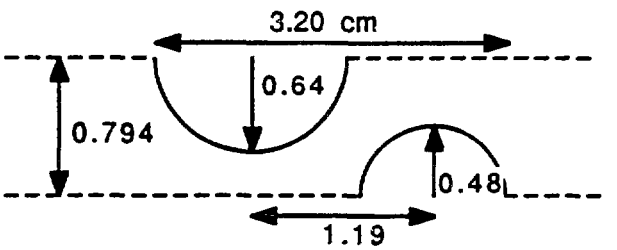

ORNL C-MOD (Shield #10)

(Hoffman, et al, Fusion Tech 8, p 392)

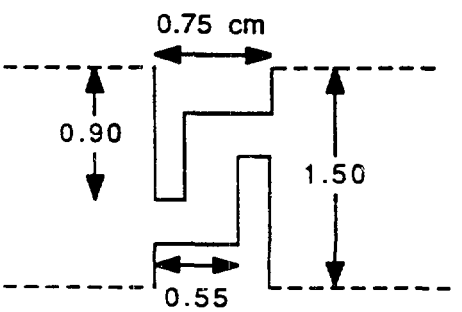

"ASDEX"

(Hoffman, et al, Fusion Tech 8, p 392)

Fig. 1

TYPICAL CAVITY GEOMETRY FOR FARADAY SHIELD CALCULATIONS

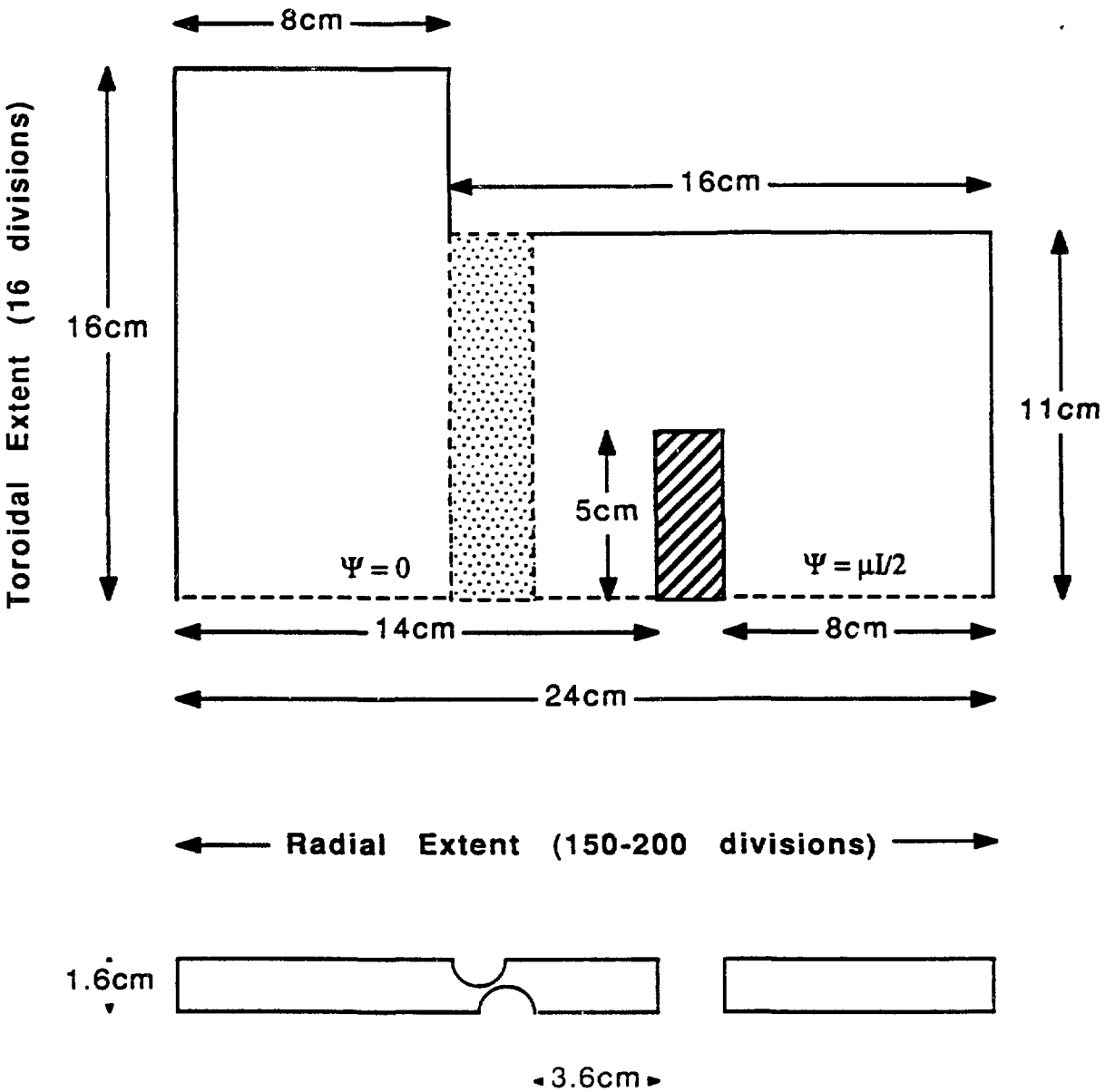

The poloidal extent (20-25 divisions) is one Faraday shield period

Fig. 2

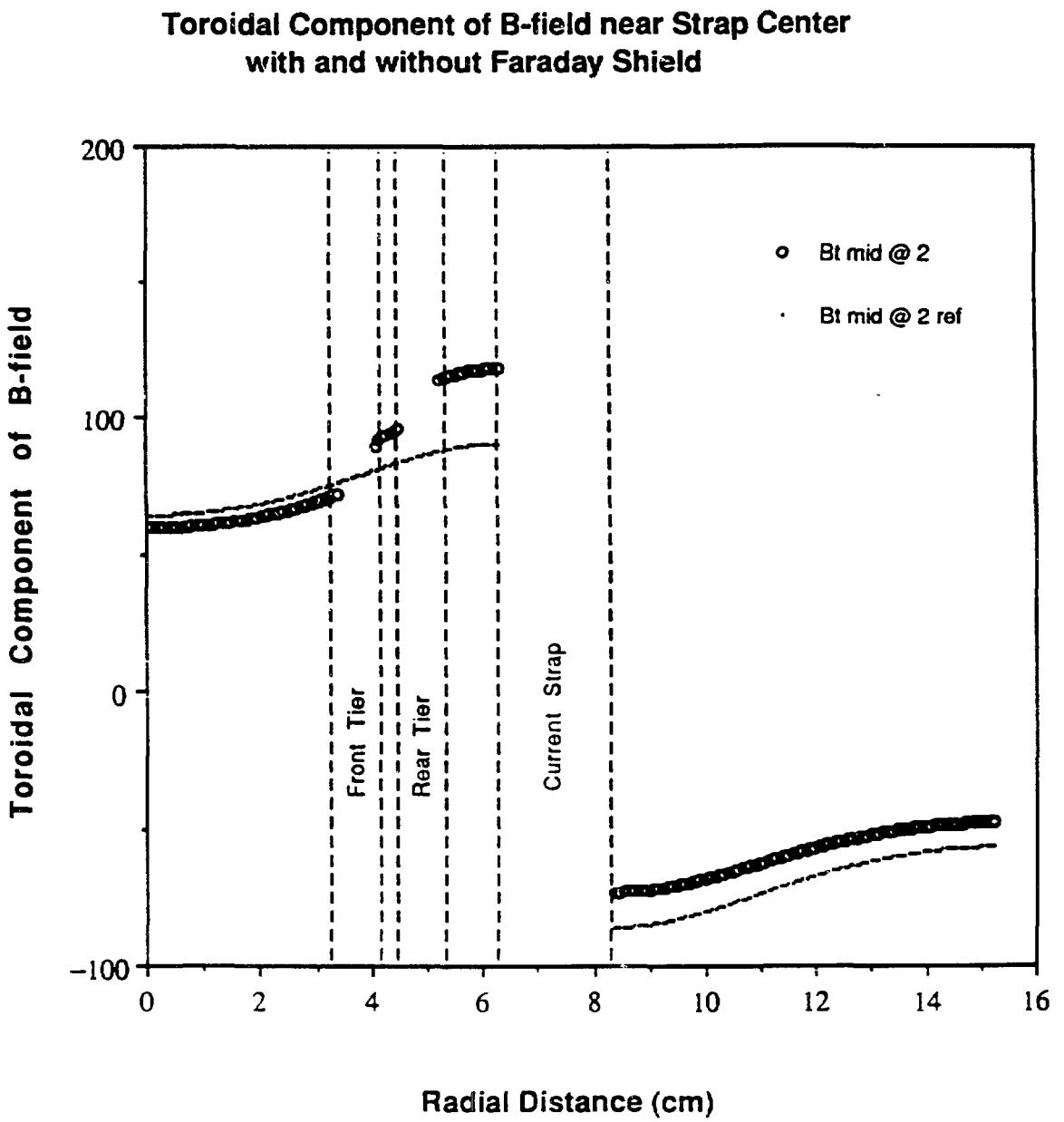
Toroidal Component of B-field near Strap Center
with and without Faraday Shield
Toroidal Component of B-field
Radial Distance (cm)
Bt mid @ 2
Bt mid @ 2 ref
Front Tier
Rear Tier
Current Strap
200
100
0
−100
0
2
4
6
8
10
12
14
16

Fig. 3a

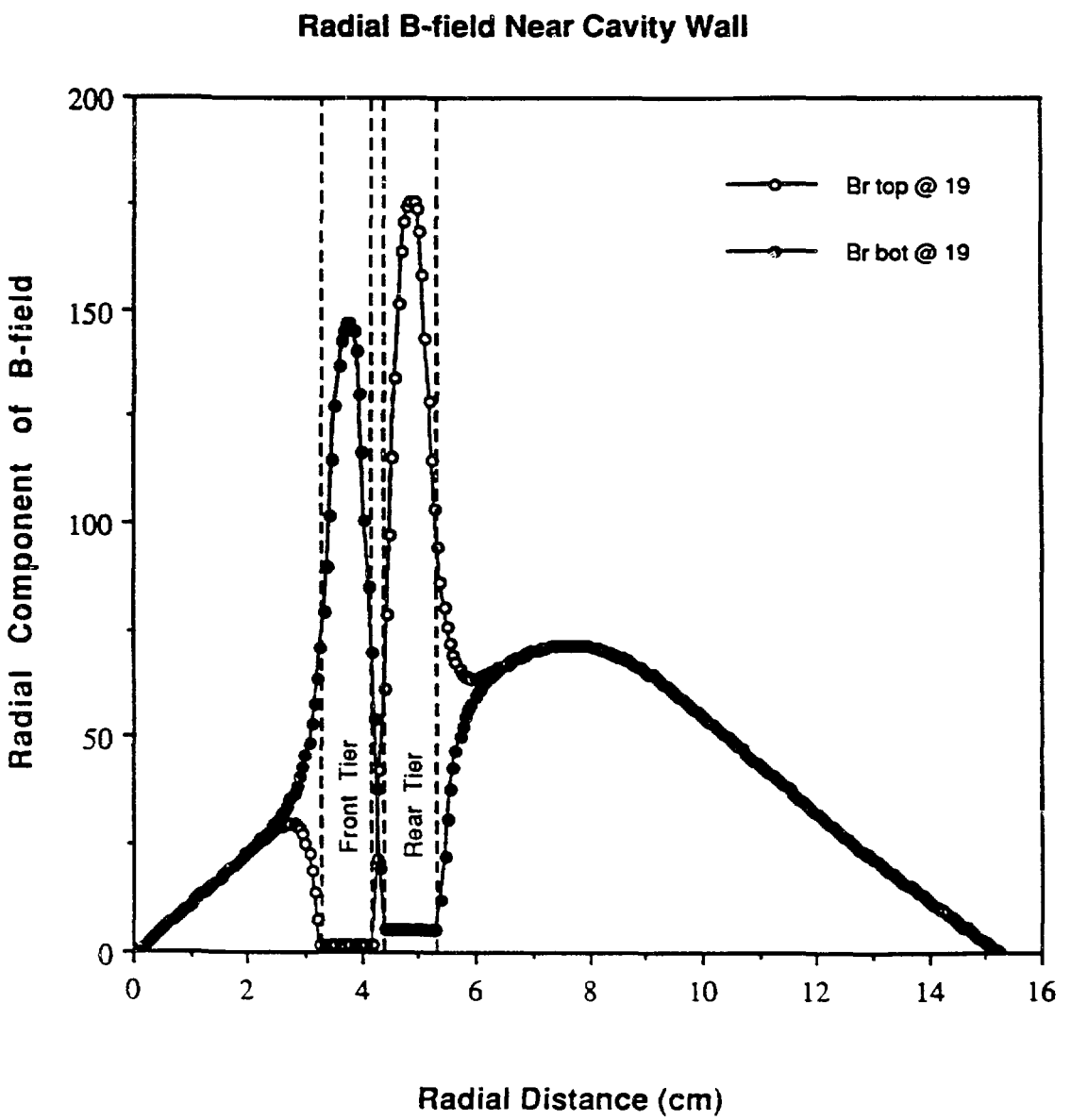
Radial B-field Near Cavity Wall
Radial Component of B-field
Radial Distance (cm)
Br top @ 19
Br bot @ 19
Front Tier
Rear Tier
200
150
100
50
0
0
2
4
6
8
10
12
14
16

Fig. 3b

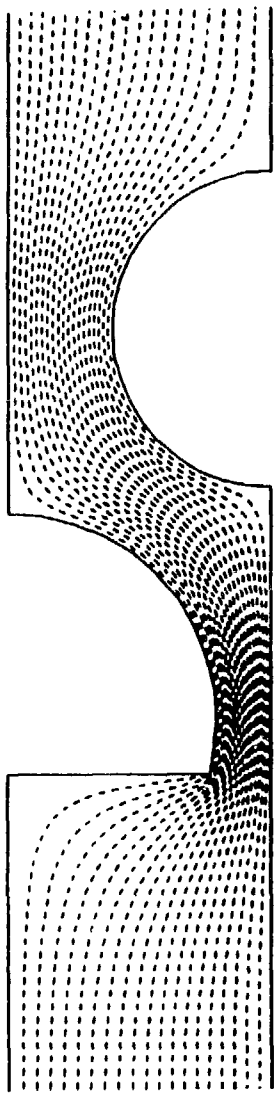

Fig. 4

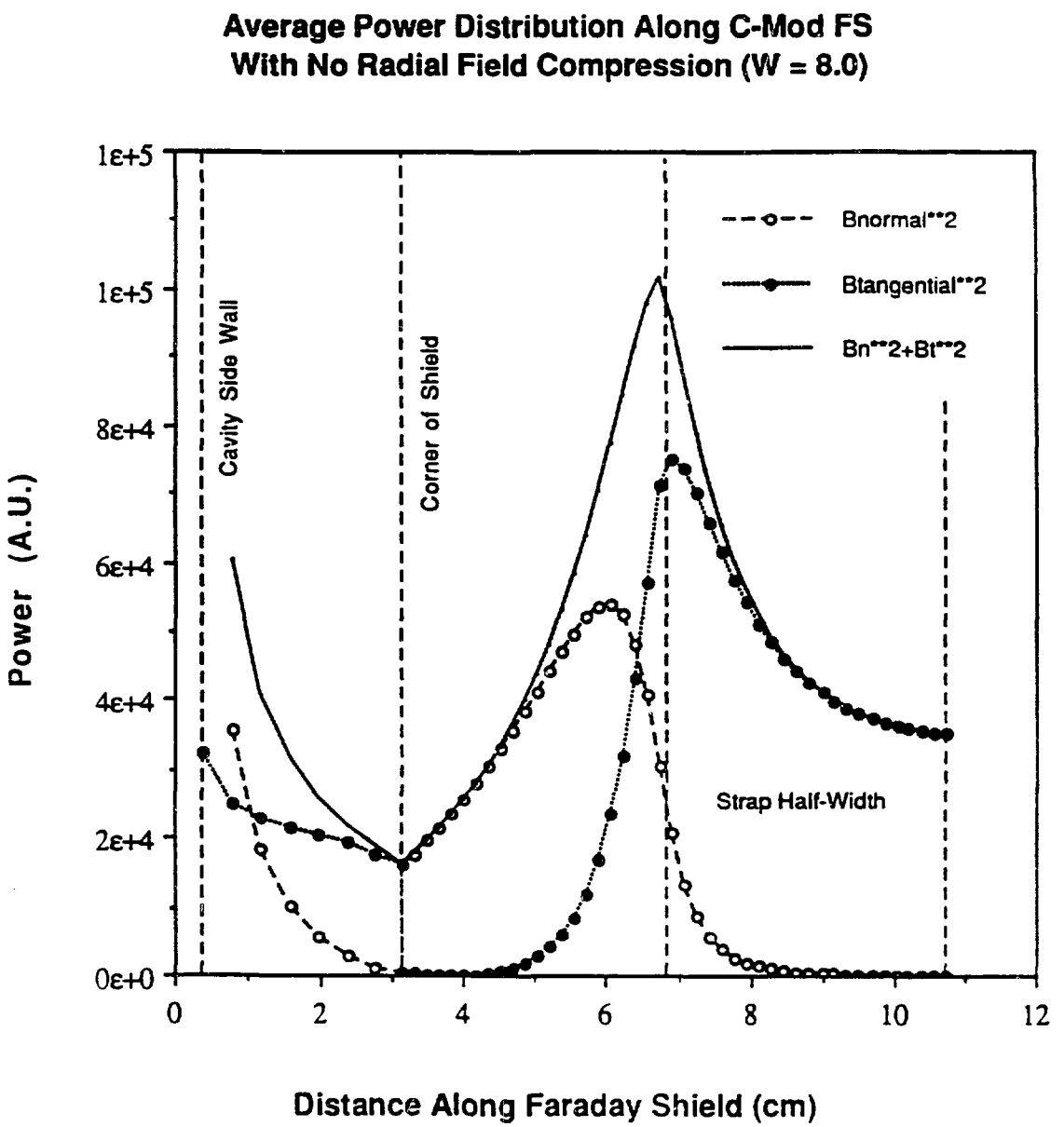
Average Power Distribution Along C-Mod FS
With No Radial Field Compression (W = 8.0)
Power (A.U.)
1ε+5
1ε+5
8ε+4
6ε+4
4ε+4
2ε+4
0ε+0
0
2
4
6
8
10
12
Distance Along Faraday Shield (cm)
Cavity Side Wall
Corner of Shield
Strap Half-Width
Bnormal**2
Btangential**2
Bn**2+Bt**2

Fig. 5a

Average Power Distribution Along C-Mod FS
With Radial Compression (Flattened Front)

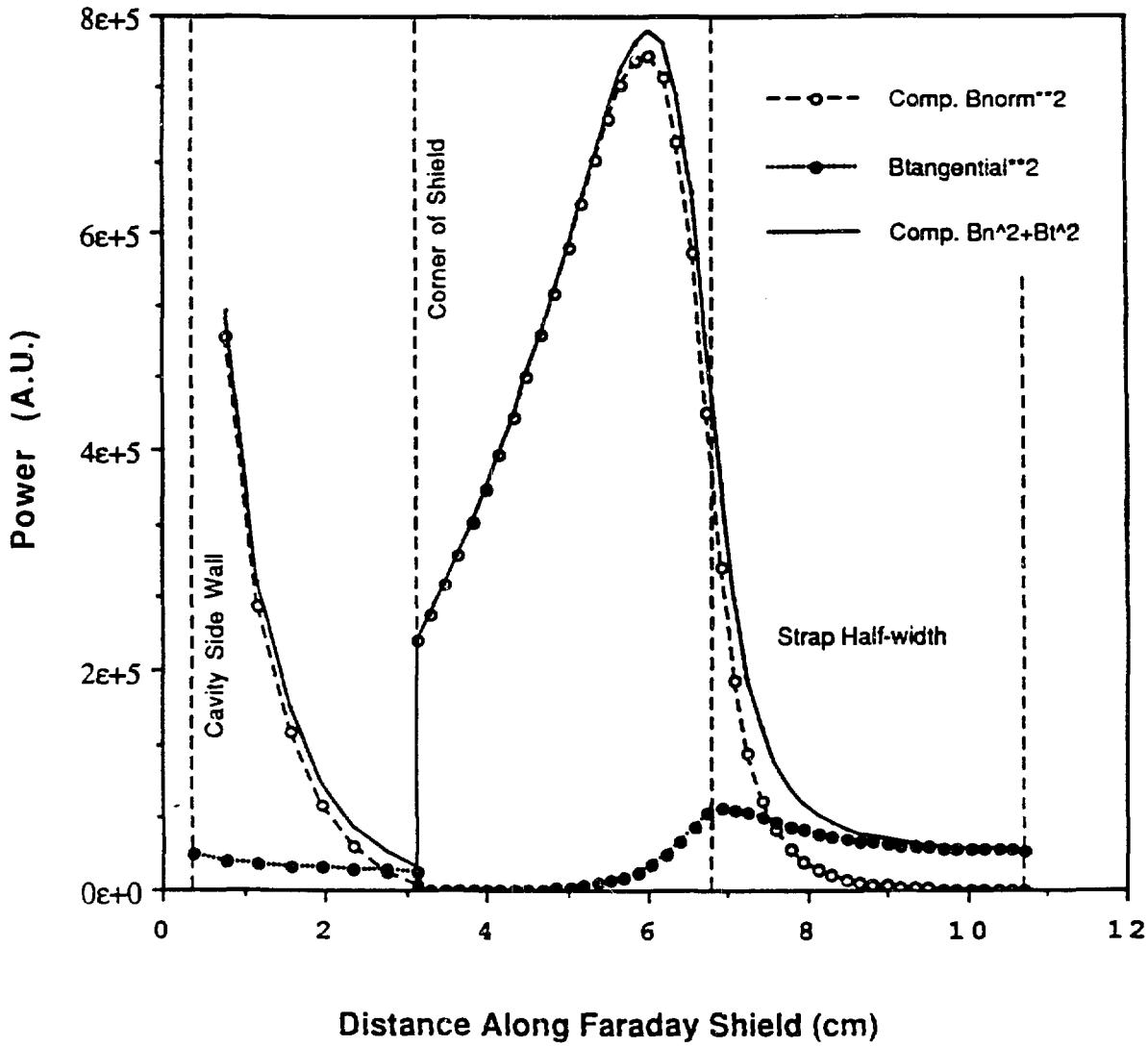

Fig. 5b

CONF-8910225--2

"The submitted manuscript has been authored by a contractor of the U.S. Government under contract No. DE-AC05-84OR21400. Accordingly, the U.S. Government retains a nonexclusive, royalty-free license to publish or reproduce the published form of this contribution, or allow others to do so, for U.S. Government purposes."

Determination of ICRF Antenna Fields in the Vicinity of a 3-D Faraday Shield Structure

P.M. Ryan,
K.E. Rothe, J.H. Whealton, T.D. Shepard

Oak Ridge National Laboratory
Oak Ridge, TN 37830, USA

IAEA Technical Committee Meeting
on ICRH/Edge Physics
Garching, West Germany
2-5 October 1989

DISCLAIMER

This report was prepared as an account of work sponsored by an agency of the United States Government. Neither the United States Government nor any agency thereof, nor any of their employees, makes any warranty, express or implied, or assumes any legal liability or responsibility for the accuracy, completeness, or usefulness of any information, apparatus, product, or process disclosed, or represents that its use would not infringe privately owned rights. Reference herein to any specific commercial product, process, or service by trade name, trademark, manufacturer, or otherwise does not necessarily constitute or imply its endorsement, recommendation, or favoring by the United States Government or any agency thereof. The views and opinions of authors expressed herein do not necessarily state or reflect those of the United States Government or any agency thereof.

MASTER

DISTRIBUTION OF THIS DOCUMENT IS UNLIMITED

The motivation behind this work was to develop a numerical tool to aid in evaluating Faraday shield designs.

Need to determine:

- Transmission Coefficients
- Effect of the Shield on Antenna Inductance and Capacitance
- Power Dissipation in the Shield

3D MODEL USING MAGNETIC SCALAR POTENTIAL

$$\nabla\times\mathbf{B} = \mu_0\mathbf{J} + j\omega\mu_0\varepsilon_0\mathbf{E} = j(k_0/c)\mathbf{E}$$

Since all currents are carried by metallic walls, $\mathbf{J} = 0$ in the current-free volume, and the long wavelength approximation (valid when $k_0/k \approx h/\lambda \ll 1$) allows the time-derivative of **E** to be neglected:

$$\nabla \times \mathbf{B} = 0$$

$$\therefore\ \mathbf{B} \equiv -\nabla\Phi_m$$

where Φ_m, the magnetic scalar potential, is a solution of Laplace's equation:

$$\nabla\bullet\mathbf{B} = \nabla\bullet(-\nabla\Phi_m) = -\nabla^2\Phi_m = 0$$

$$\oint_C \mathbf{B}\bullet d\mathbf{l} = \mu_0\int_S \mathbf{J}\bullet d\mathbf{s} = \mu_0 I_{strap}$$

$$\oint_C \mathbf{B}\bullet d\mathbf{l} = \oint_C -\nabla\Phi_m\, d\mathbf{l} = 2\int_{C/2} -\nabla\Phi_m\, d\mathbf{l} = 2(\Phi_{m1}-\Phi_{m2})$$

Boundary Conditions for Laplace's Equation

Dirichlet BC on the symmetry planes of current strap:

$$\Phi_{m2} = 0 \quad\Rightarrow\quad \Phi_{m1} = \frac{\mu_0 I_{strap}}{2}$$

Neumann BC on metallic surfaces:

$$\hat{\mathbf{n}}\bullet\mathbf{B} = \hat{\mathbf{n}}\bullet\nabla\Phi_m = \frac{\partial\Phi_m}{\partial\hat{\mathbf{n}}} = 0$$

PMRyan 3 Oct 89

TYPICAL CAVITY GEOMETRY FOR FARADAY SHIELD CALCULATIONS

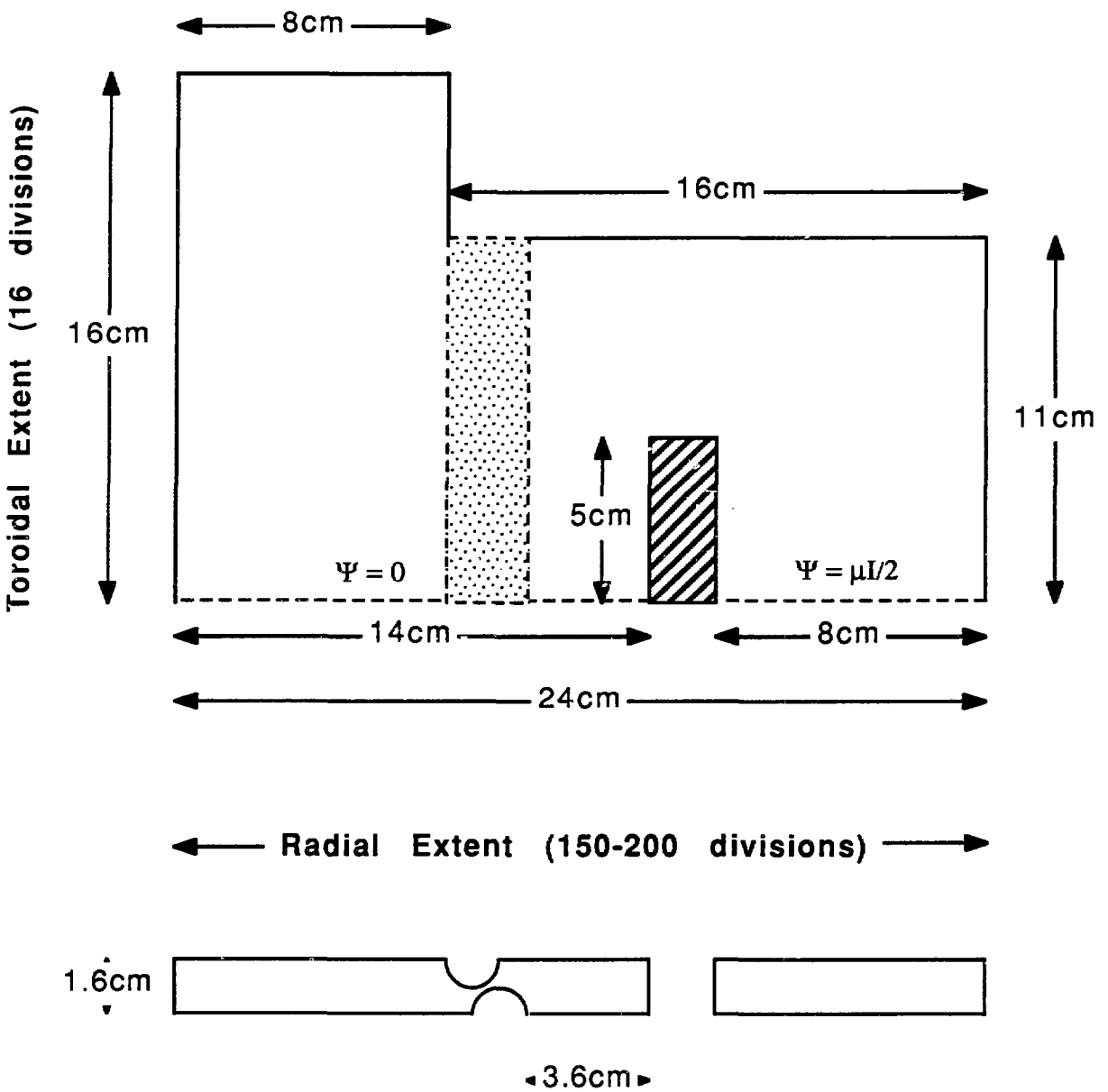

The poloidal extent (20-25 divisions) is one Faraday shield period

Fig. 3

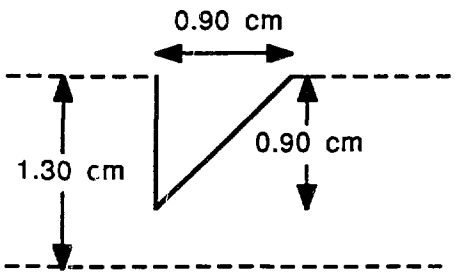

SINGLE TIER TRIANGULAR

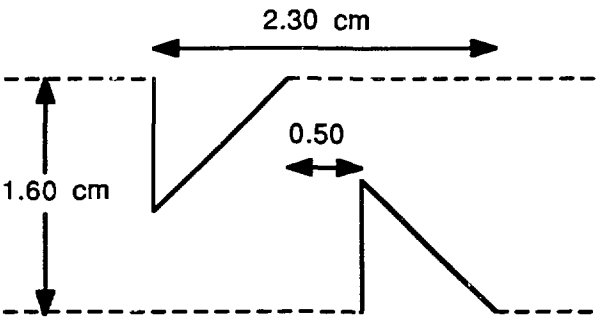

DOUBLE TIER "PERKINS"

(Perkins, PPPL Report 2571)

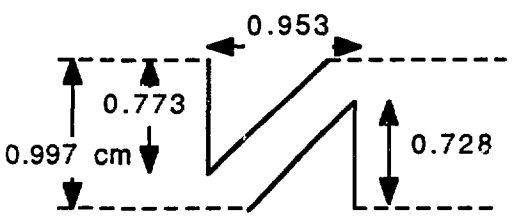

MIT C-MOD

(Takase, et al, AIP Conf 190, p. 346)

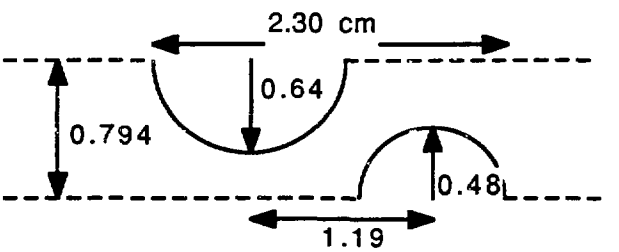

ORNL C-MOD (Shield #10)

(Hoffman, et al, Fusion Tech 8, p 392)

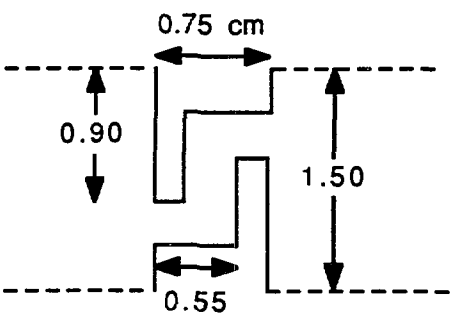

"ASDEX"

(Hoffman, et al, Fusion Tech 8, p 392)

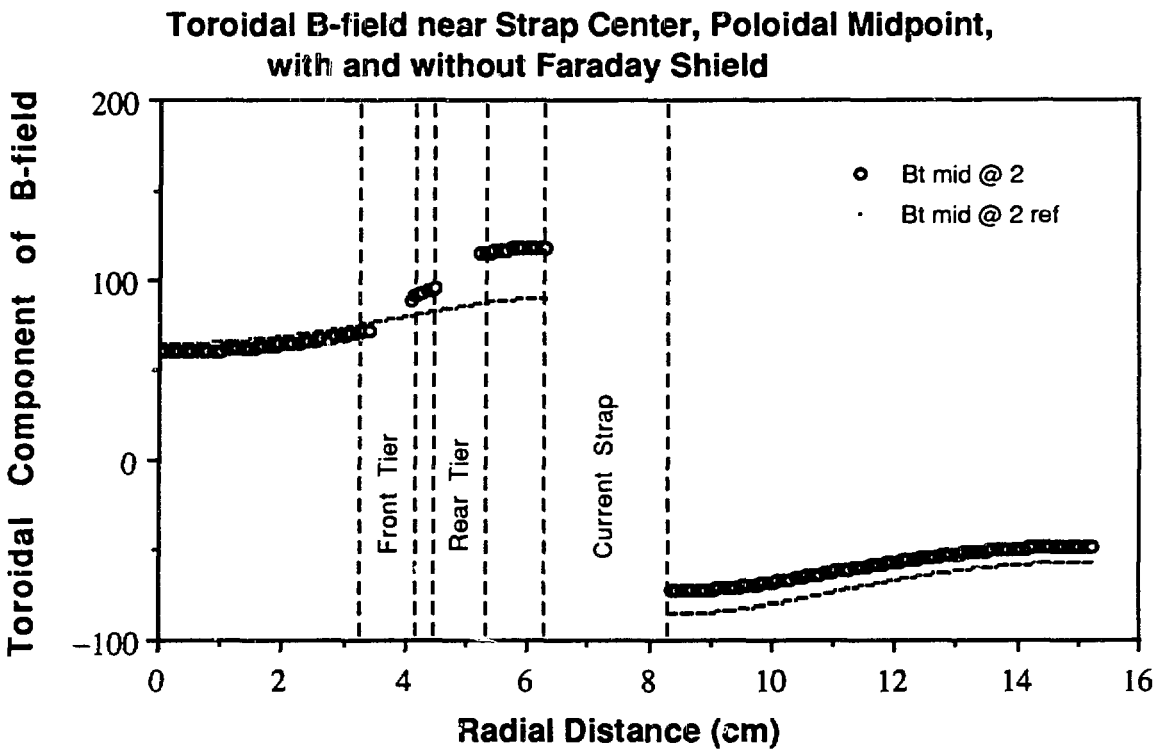
Toroidal B-field near Strap Center, Poloidal Midpoint,
with and without Faraday Shield
Toroidal Component of B-field
200
100
0
−100
0
2
4
6
8
10
12
14
16
Radial Distance (cm)
Front Tier
Rear Tier
Current Strap
Bt mid @ 2
Bt mid @ 2 ref

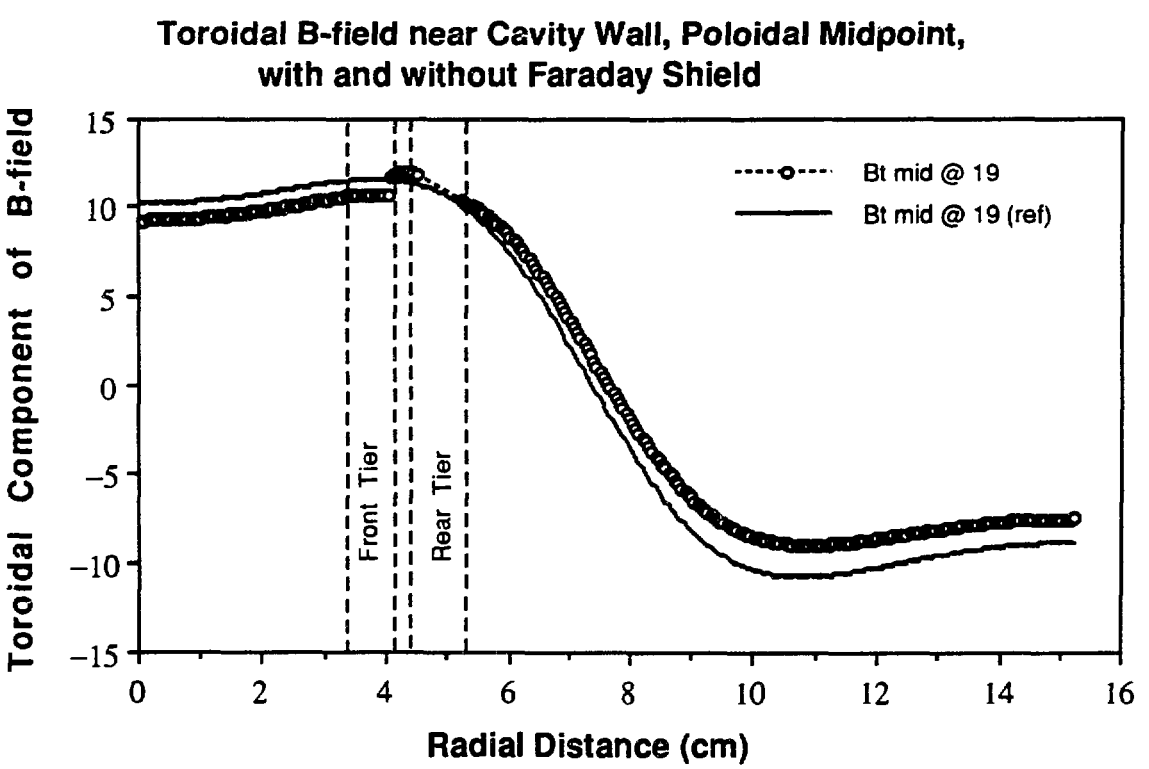
Toroidal B-field near Cavity Wall, Poloidal Midpoint,
with and without Faraday Shield
Toroidal Component of B-field
15
10
5
0
−5
−10
−15
0
2
4
6
8
10
12
14
16
Radial Distance (cm)
Front Tier
Rear Tier
Bt mid @ 19
Bt mid @ 19 (ref)

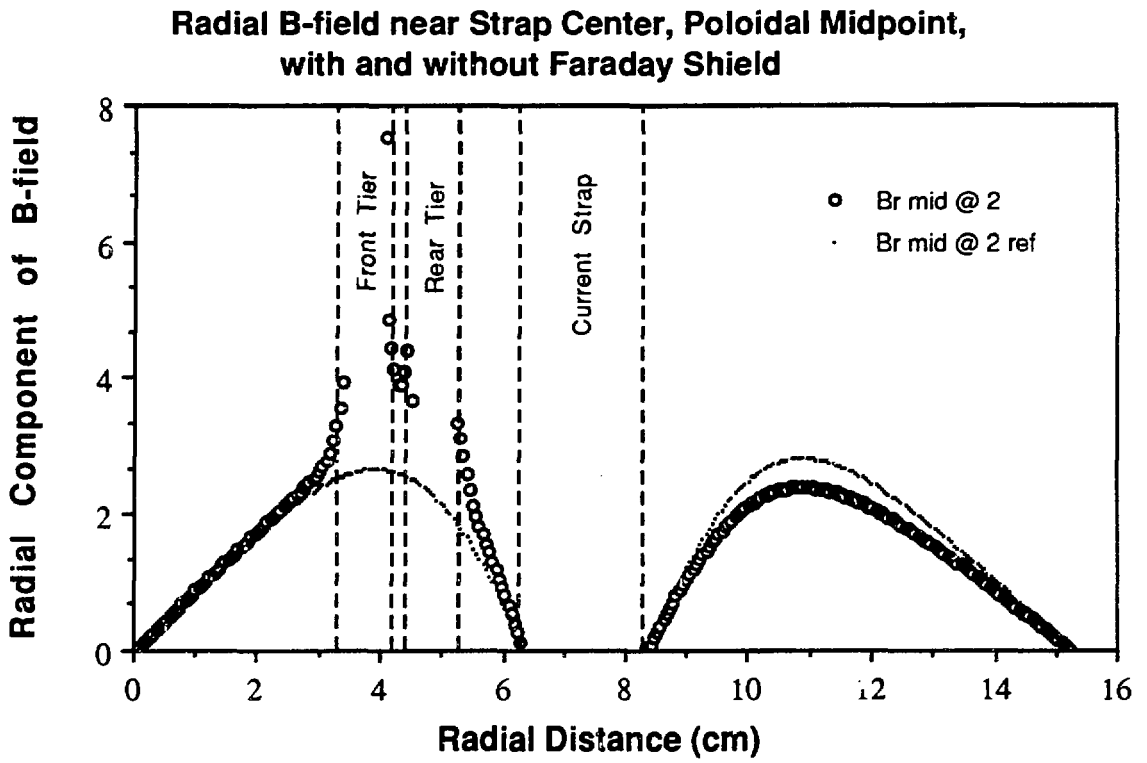
Radial B-field near Strap Center, Poloidal Midpoint,
with and without Faraday Shield
Radial Component of B-field
Radial Distance (cm)
Front Tier
Rear Tier
Current Strap
Br mid @ 2
Br mid @ 2 ref
0
2
4
6
8
10
12
14
16

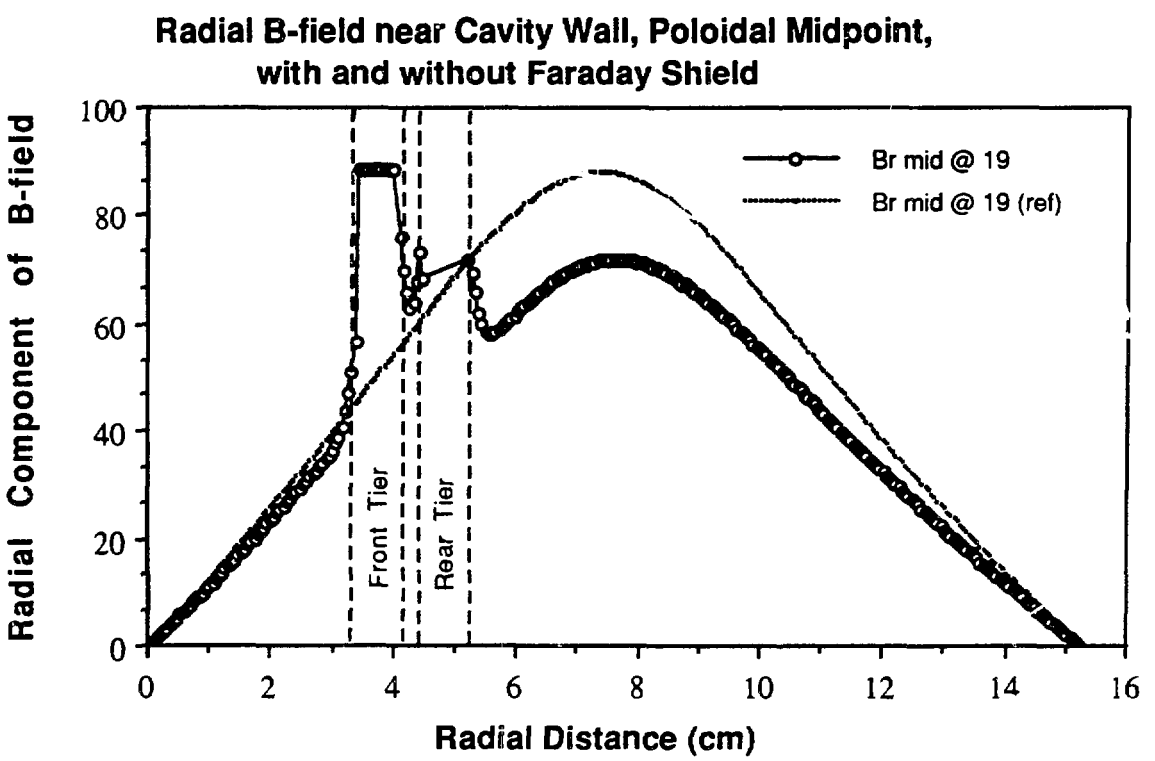
Radial B-field near Cavity Wall, Poloidal Midpoint,
with and without Faraday Shield
Radial Component of B-field
Radial Distance (cm)
Front Tier
Rear Tier
Br mid @ 19
Br mid @ 19 (ref)
0
20
40
60
80
100
2
4
6
8
10
12
14
16

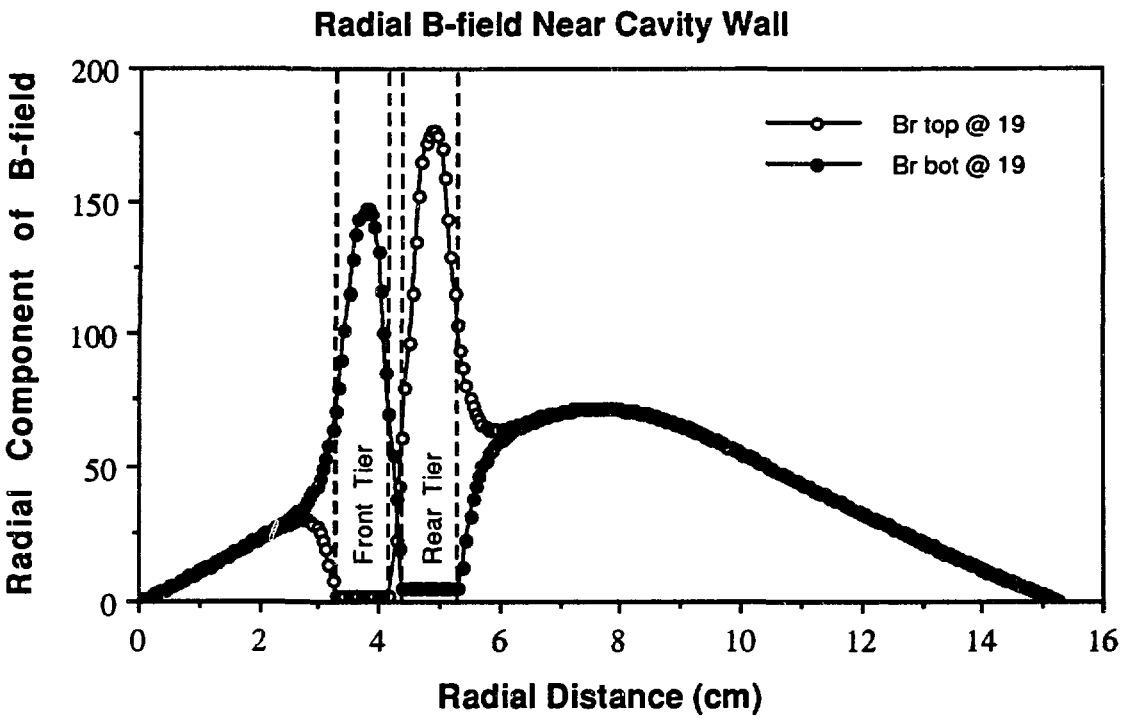
Radial B-field Near Cavity Wall
Radial Component of B-field
Radial Distance (cm)
Br top @ 19
Br bot @ 19
Front Tier
Rear Tier
200
150
100
50
0
0
2
4
6
8
10
12
14
16

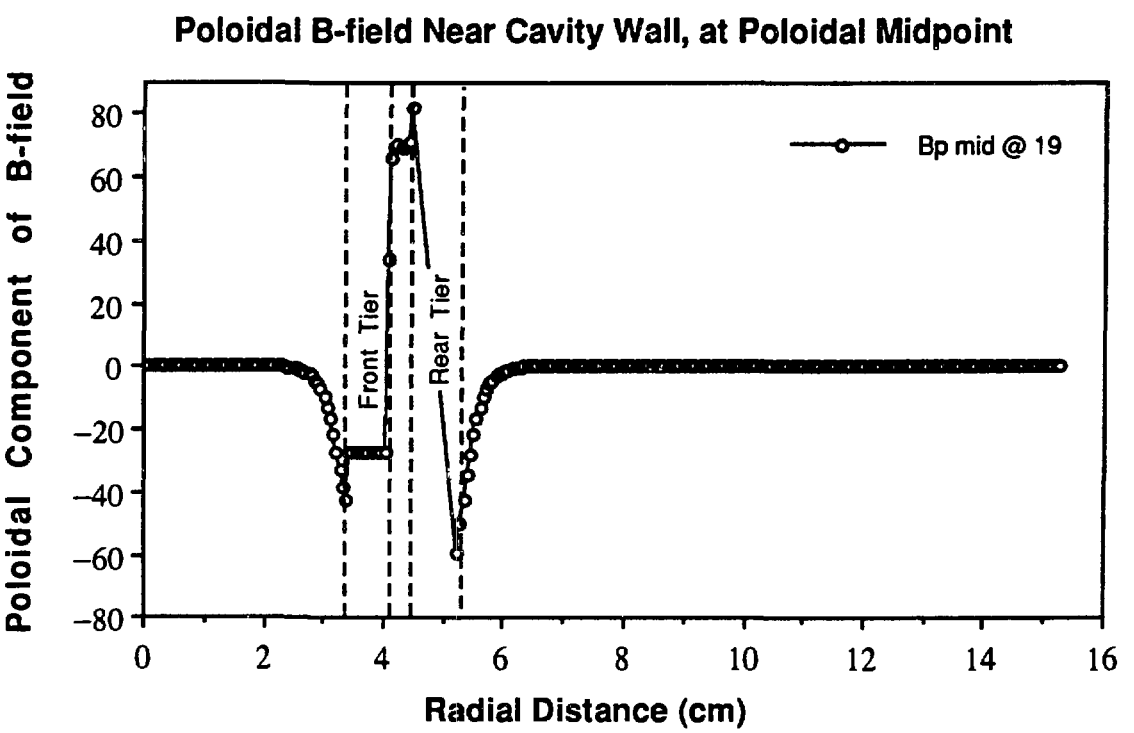
Poloidal B-field Near Cavity Wall, at Poloidal Midpoint
Poloidal Component of B-field
Radial Distance (cm)
Bp mid @ 19
Front Tier
Rear Tier
80
60
40
20
0
−20
−40
−60
−80
0
2
4
6
8
10
12
14
16

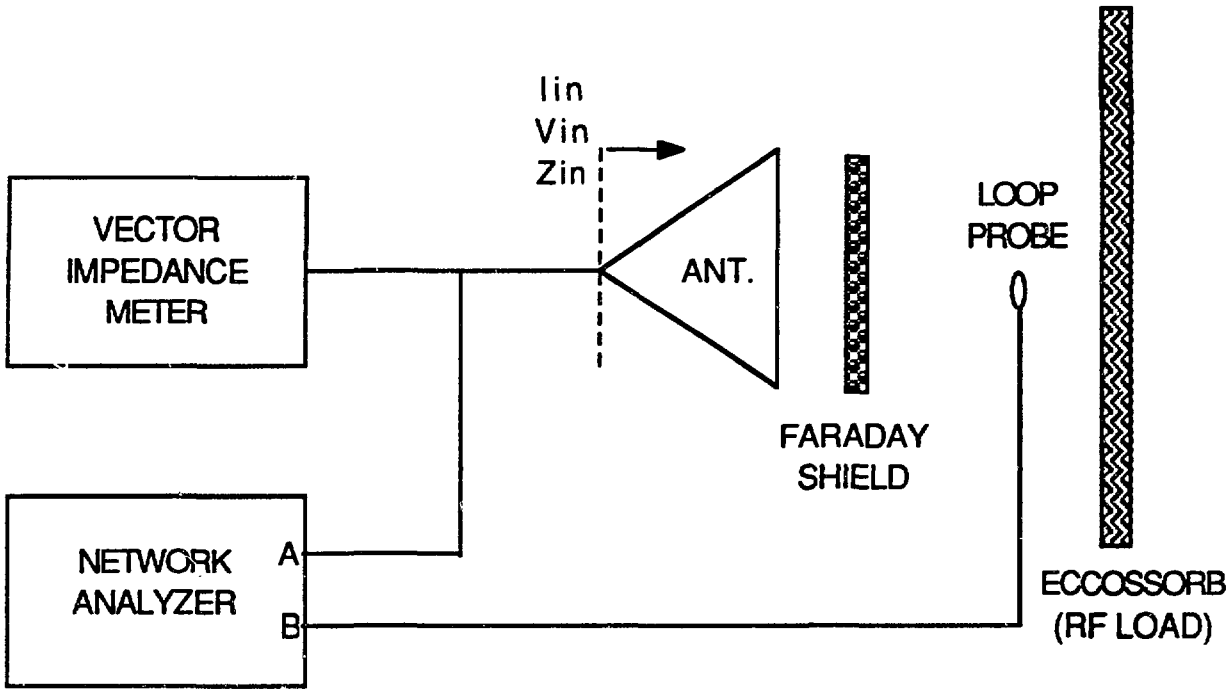

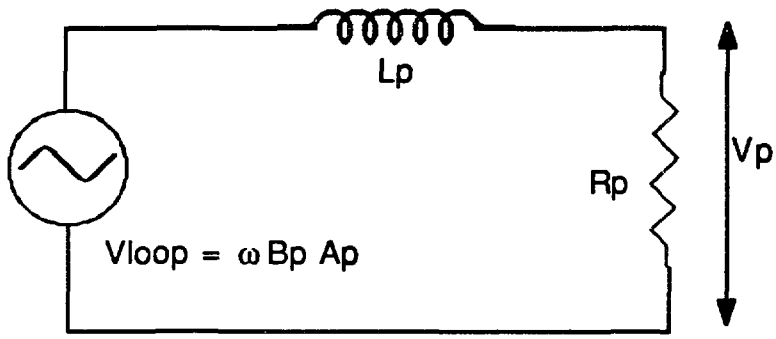

$$(Tp)eff = (Tp) - Rfs/Rload$$

PMRyan 3 Oct 89

COMPARISON OF CALCULATIONS WITH MEASUREMENTS

GEOMETRY	SINGLE TIER TRIANGULAR	DOUBLE TIER "PERKINS"	ORNL CMOD (Shield #10)	MIT CMOD	"ASDEX"
Transmission (T)					
Measured	0.804	0.749	0.897	-	0.767
Calculated	0.883	0.835	0.915	0.819	0.831
Power Trans. (T^2)					
Measured	0.646	0.561	0.805	-	0.588
Calculated	0.775	0.697	0.840	0.667	0.687
Effective	0.718	0.583	-	-	-
$\Delta L'/L'$					
Measured	-3.0%	-3.7%	-7.5%	-	-9.6%
Calculated	-1.3%	-1.8%	-9.0%	-15.7%	-8.1%
$\Delta C'/C'$					
Calculated	+24.5%	+23.4%	+109%	-	-

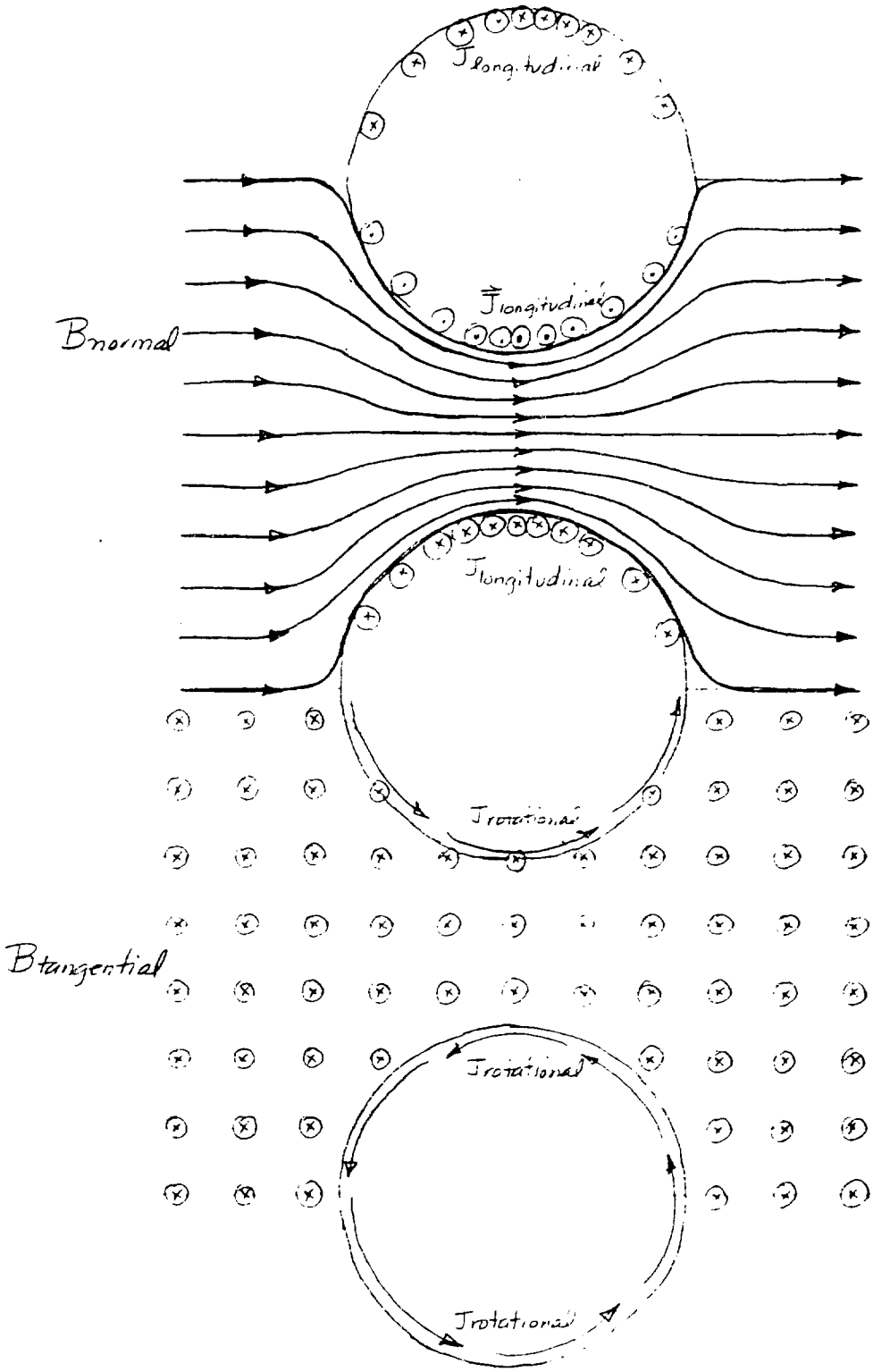
J longitudinal
J longitudinal
B normal
J longitudinal
J rotational
B tangential
J rotational
J rotational

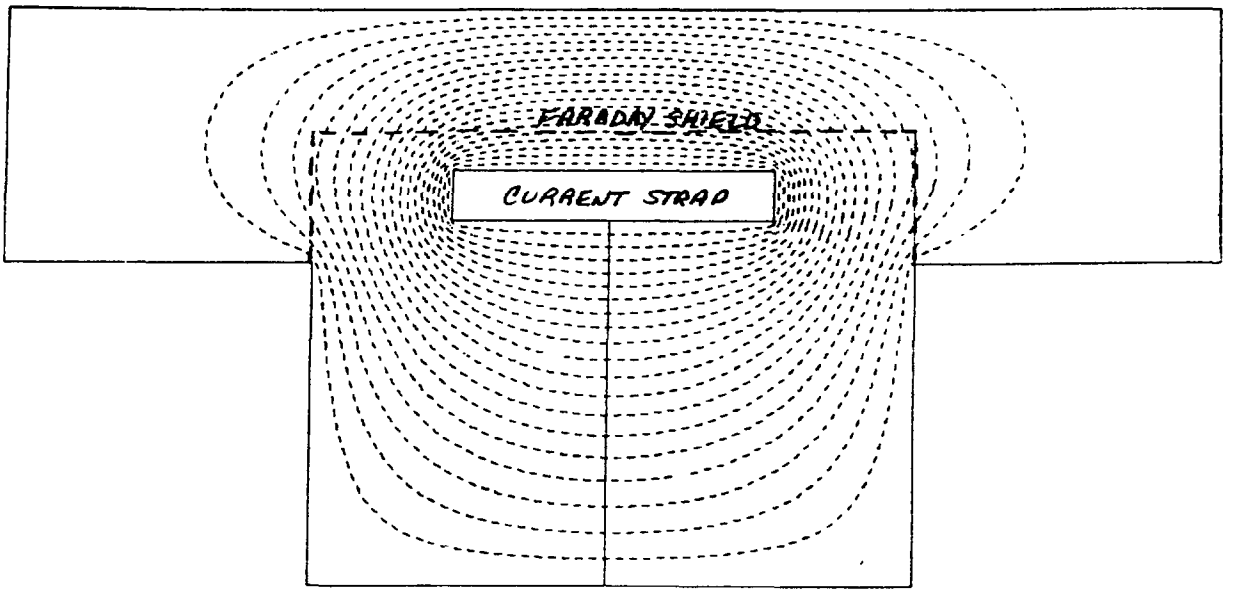
FARADAY SHIELD
CURRENT STRAP

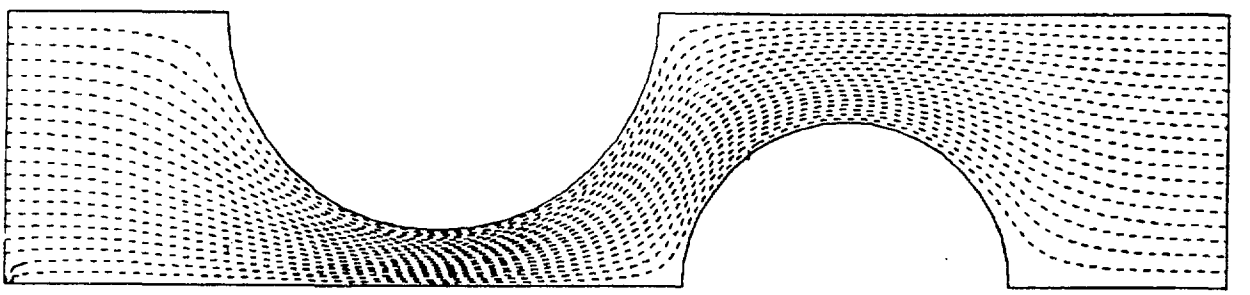

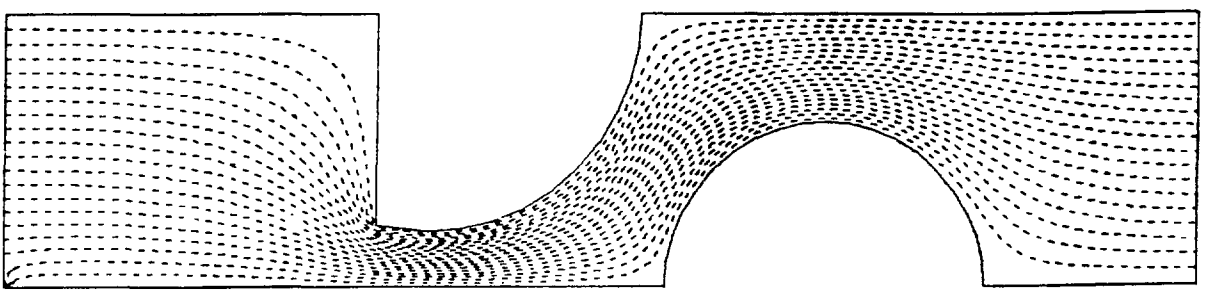

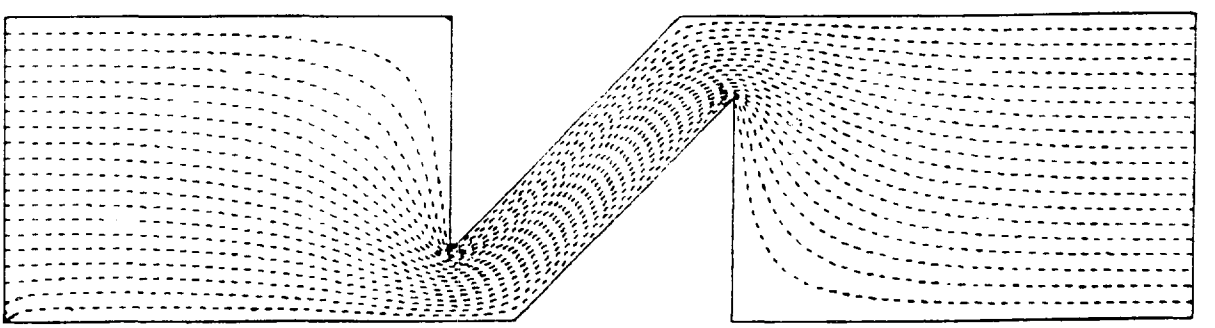

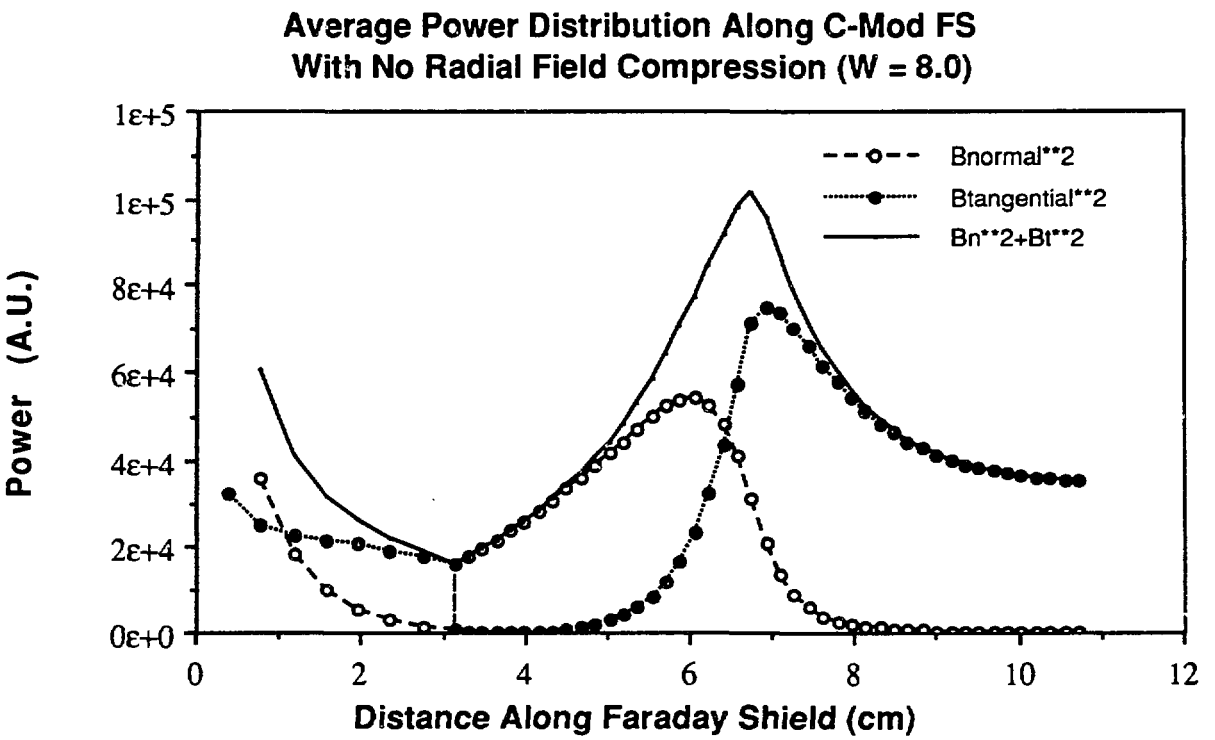
Average Power Distribution Along C-Mod FS
With No Radial Field Compression (W = 8.0)
Power (A.U.)
1ε+5
1ε+5
8ε+4
6ε+4
4ε+4
2ε+4
0ε+0
0
2
4
6
8
10
12
Distance Along Faraday Shield (cm)
Bnormal**2
Btangential**2
Bn**2+Bt**2

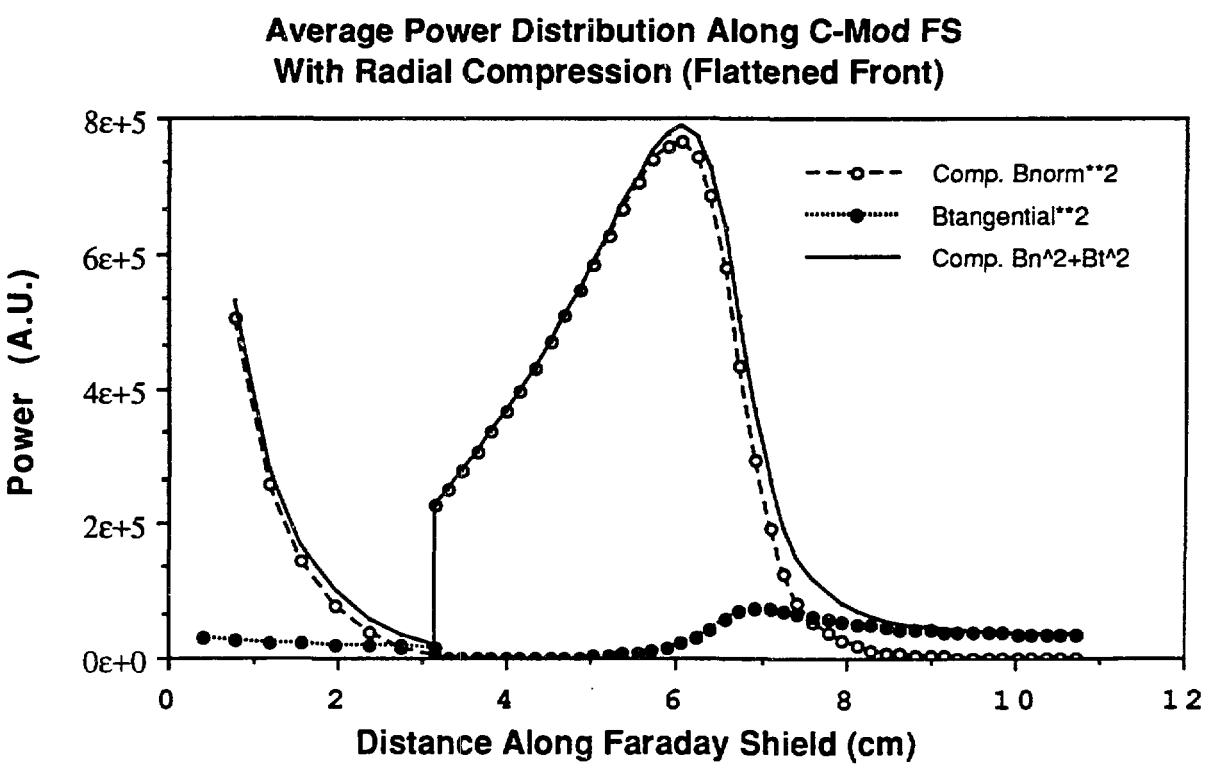
Average Power Distribution Along C-Mod FS
With Radial Compression (Flattened Front)
Power (A.U.)
8ε+5
6ε+5
4ε+5
2ε+5
0ε+0
0
2
4
6
8
10
12
Distance Along Faraday Shield (cm)
Comp. Bnorm**2
Btangential**2
Comp. Bn^2+Bt^2